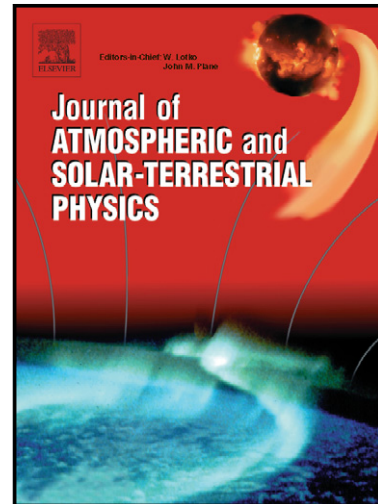


Author's Accepted Manuscript

Estimating the Lower Ionosphere Height and
Lightning Location using Multimode "Tweek"
Atmospherics

A.V. Shvets, T.M. Serdiuk, Y.V. Gorishnyaya, Y.
Hobara, M. Hayakawa



www.elsevier.com/locate/jastp

PII: S1364-6826(13)00306-4
DOI: <http://dx.doi.org/10.1016/j.jastp.2013.11.007>
Reference: ATP3944

To appear in: *Journal of Atmospheric and Solar-Terrestrial Physics*

Received date: 6 February 2013

Revised date: 9 September 2013

Accepted date: 13 November 2013

Cite this article as: A.V. Shvets, T.M. Serdiuk, Y.V. Gorishnyaya, Y. Hobara, M. Hayakawa, Estimating the Lower Ionosphere Height and Lightning Location using Multimode "Tweek" Atmospherics, *Journal of Atmospheric and Solar-Terrestrial Physics*, <http://dx.doi.org/10.1016/j.jastp.2013.11.007>

This is a PDF file of an unedited manuscript that has been accepted for publication. As a service to our customers we are providing this early version of the manuscript. The manuscript will undergo copyediting, typesetting, and review of the resulting galley proof before it is published in its final citable form. Please note that during the production process errors may be discovered which could affect the content, and all legal disclaimers that apply to the journal pertain.

1 ESTIMATING THE LOWER IONOSPHERE HEIGHT AND LIGHTNING LOCATION USING
2 MULTIMODE "TWEAK" ATMOSPHERICS

3
4 A.V. Shvets¹, T.M. Serdiuk², Y.V. Gorishnyaya¹, Y. Hobara³, and M. Hayakawa³

5
6 ¹ O. Ya. Usikov Institute for Radiophysics and Electronics, of the National Academy of Sciences of
7 Ukraine, 12 Akademika Proskury St., Kharkov 61085, Ukraine

8 ² Lazaryan's National University of Railway Transport, 2a Akademika Lazaryana St.,
9 Dnepropetrovsk 49010, Ukraine

10 ³ The University of Electro-Communications, 1-5-1 Chofugaoka, Chofu Tokyo, 182-8585, Japan

11
12 Abstract There is proposed a new method of estimating the effective ionospheric height of the
13 Earth-ionosphere waveguide and the propagation distance of tweak-atmospherics. It is based on the
14 compensation of waveguide frequency dispersion of a tweak signal, which enables us to improve the
15 accuracy of deducing the cutoff frequencies, especially in the presence of noise. An approach to solve
16 the inverse problem is suggested that reduces the task of finding both the source range and the
17 waveguide cutoff frequencies by using the multimode characteristics of tweaks to an issue of one-
18 dimensional optimization. Based on the numerical modeling of multimode tweak-atmospherics in the
19 Earth-ionosphere waveguide with exponential vertical conductivity profile of the lower ionosphere, it
20 was shown that the accuracy of estimating the effective waveguide height by the new method is good
21 as about 100-400 m for the first and higher order modes. It then allows us to estimate the parameters
22 of vertical conductivity profile of the lower ionosphere for a wide range of source distances from a
23 few hundred to a few thousand kilometers, as long as two or more tweak harmonics can be detected.
24 Preliminary analysis of experimental tweak records show a decrease of the effective height with
25 increasing the mode number, and the scale height of the exponential vertical conductivity profile for
26 the isotropic lower ionosphere model is estimated to be in a range of 0.4 – 2.5 km.

27

28 *Keywords:* Earth-ionosphere waveguide, tweek-atmospherics, lightning location, lower
29 ionosphere diagnostics.

30

31 1. Introduction

32 Tweek-atmospherics are electromagnetic pulses with duration of 10 – 100 milliseconds,
33 propagating in the natural Earth-ionosphere waveguide, which represent a response of the natural
34 cavity to lightning discharges. These tweeks are formed due to small losses during night time in the
35 ionosphere at altitudes from about 85 to 95 km, which effectively reflects ELF-VLF electromagnetic
36 waves. A study of this altitude range in the ionosphere meets essential difficulties due to relatively
37 small electron densities ($10 - 1000 \text{ cm}^{-3}$), and so these tweeks are considered to be a useful natural
38 means for radiosounding the lower ionosphere in a wide frequency band.

39 Approximation of a flat infinite waveguide with perfectly conducting walls is known to quite
40 well describe the waveguide dispersion effects observed in the experiment, especially near the cutoff
41 frequencies [*Otsu*, 1960]. Based on the waveguide propagation theory, different methods of analysis
42 of tweeks were elaborated to estimate the lower ionosphere effective height, together with the
43 propagation distance. Analyses of instant frequency variations of tweek signals [*Otsu*, 1960; *Yano et*
44 *al.*, 1989; *Shimakura et al.*, 1992; *Hayakawa et al.*, 1994, 1995; *Ohya et al.*, 2008], phase spectrum of
45 the longitudinal magnetic field component [*Rafalsky et al.*, 1995], interference between the zeroth and
46 the first order modes in the tweek amplitude spectrum [*Shvets and Gorishnyaya*, 2010] were
47 employed in the frequency domain around the first waveguide cutoff frequency to find both the
48 effective waveguide height and source-to-observer distance. Further spectral peculiarities of long-
49 range tweek atmospherics were studied theoretically and experimentally in *Mikhailova and Kapustina*
50 (1988), and *Yedemsky et al.* (1992). But scarce attention was devoted experimentally to the use of
51 multimode tweeks that represent the higher order modes of the Earth-ionosphere waveguide, except

52 some numerical studies [Cummer *et al.*, 1998; Cummer, 2000] in which they extended the frequency
53 range of analysis and obtained more detailed information on the lower ionosphere.

54 The cutoff frequency defined for a particular waveguide mode can be related to a certain
55 altitude in the ionosphere which can be considered as an effective waveguide height. Because the
56 depth of penetration of electromagnetic waves into the ionospheric plasma depends on wave
57 frequency, the effective waveguide height is known to change for different modes. So, determination
58 of the cutoff frequencies for higher order modes of the Earth-ionosphere waveguide by using tweek
59 atmospherics, will provide us with the detailed parameters of the lower ionosphere.

60 An approximate theory has been developed which describes the tweek formation under an
61 anisotropic, both homogeneous [Yedemsky *et al.*, 1992; Ryabov, 1992; Sukhorukov *et al.*, 1992a] and
62 inhomogeneous [Sukhorukov *et al.*, 1992b], ionosphere near the cutoff frequencies. These theories
63 predict the deeper penetration of the lower frequency waves into the ionosphere that leads to a
64 decrease in the effective reflection height for higher order modes. The similar behavior for the higher
65 order modes is also obtained from the simplified theory [Porrat *et al.*, 2001] based on the model of an
66 exponential vertical conductivity profile of the isotropic lower ionosphere, which describes
67 satisfactorily spectral peculiarities of nighttime atmospherics in the frequency range up to 5 kHz.
68 Shvets and Hayakawa (1998) considered the altitude where the full reflection condition is fulfilled in
69 the nighttime ionosphere for the extraordinary left-hand polarized waves, which form tweeks near the
70 cutoff frequencies [Hayakawa *et al.*, 1994]. It implies that the effective height increases with an
71 increase in the mode number. This was confirmed by our initial estimations [Shvets and Hayakawa,
72 1998] and by recent experimental studies of the higher harmonic tweeks (see e.g. Maurya *et al.*,
73 [2012] and references therein), but it contradicts to the theoretical consequence by Ryabov (1992) and
74 Sukhorukov *et al.* [1992a]. Thus the evaluation of accuracy of existing techniques and development
75 of new techniques to determine the cutoff frequencies of higher harmonic tweeks is of great interest in
76 interpreting the experimental data.

77 The waveform of tweeks in the range of waveguide cutoff frequencies at ELF-VLF is resulted
78 mainly from the dispersion properties of the Earth-ionosphere waveguide and the propagation
79 distance. While the amplitude spectrum of a tweek exhibits a complicated structure due to the result
80 of interference between different waveguide modes and depends on the distance, its dynamic
81 spectrum enhances the temporal evolution of instantaneous frequencies of the signal so that we are
82 able to identify one to up to ten tweek harmonics corresponding to the first and higher order
83 waveguide modes.

84 The inverse problem to find the cutoff frequencies and the source range by using higher tweek
85 harmonics can be solved separately for each mode. Sometimes in the experiment it leads to confusing
86 results when estimating the source range made by different tweek harmonics, which are found to be
87 quite different even for the same tweek. We here propose an approach to solve this problem
88 simultaneously for all harmonics of a detected tweek that reduces the solution to an issue of one-
89 dimensional optimization. To improve the accuracy of deducing the cutoff frequencies with higher
90 tweek harmonics we propose a transformation that nonlinearly “stretches” a tweek waveform along
91 the time axis to compensate the waveguide dispersion for a given source range. This allows us to
92 enhance the frequency resolution of spectral analysis and hence to obtain more accurate estimations of
93 the cutoff frequencies. The techniques proposed were realized programmatically and tested by the
94 numerical simulation. Also they were applied to some examples of experimental records of tweek-
95 atmospheric.

96

97 2. Earth curvature and dispersion relations

98 We consider the formation of tweek atmospheric with taking account of the Earth's
99 curvature. The scheme of propagating rays from a source (S) to the receiver (R) between the curved
100 Earth and ionosphere boundaries is shown in Fig.1, which is based on the ray approach (Yano et al.,
101 1989). The path element of a ray propagating between the Earth surface and the ionosphere is given
102 by,

$$l_n^{sphere} = \left(a^2 + (a+h)^2 - 2a(a+h)\cos\theta_n \right)^{1/2}, \quad \theta_n = \frac{\rho}{2na}, \quad (1)$$

104 where n is the ray number, a (=6371 km) is the Earth's radius, h is the waveguide height, and ρ is
105 the source-to-observer distance along the Earth surface.

106 Using an approximation for small angular distances $\cos\theta_n \approx 1 - \frac{\theta_n^2}{2}$ and letting the Earth
107 radius a to infinity, we obtain from Eq. (1) the ray path element for the flat waveguide:

$$l_n^{flat} = \sqrt{h^2 + \left(\frac{\rho}{2n} \right)^2} \quad (2)$$

109 The total path is multiplied by $2n$ of the path element, and then the propagation time of the
110 n^{th} ray is given by:

$$t_n = \frac{2nl_n}{c}, \quad n = 1, 2, 3, \dots \quad (3)$$

112 For the flat waveguide model an analytical expression for the instant frequency can be
113 obtained from Eqs.(2,3). The time of arrival of the n^{th} ray to the observer is given by:

$$t_n = \frac{1}{c} \sqrt{(2nh)^2 + \rho^2}, \quad (4)$$

115 and its derivative by n defines the instant frequency:

$$\frac{1}{f(t_n)} = \frac{dt_n}{dn} = \frac{4nh^2}{c\sqrt{(2nh)^2 + \rho^2}}. \quad (5)$$

117 Substituting $n = \frac{1}{2h} \sqrt{(ct_n)^2 - \rho^2}$ of Eq.(5) to this equation and changing t_n to the
118 continuous time, we obtain the known dependence for the instant frequency (see e.g. *Yano et al.*,
119 1989):

$$f(t) = \frac{c}{2h} \frac{1}{\sqrt{1 - \left(\frac{\rho}{ct} \right)^2}} \quad (6)$$

121 This expression is obtained also from the frequency dispersion relation for the group velocity
122 of the first waveguide mode [*Hayakawa et al.*, 1985]. The waveguide mode theory yields that the

123 value $f_c = c/(2h)$ in Eq.(6) is the cutoff frequency of the first mode. The cutoff frequency for higher
 124 order modes can be simply obtained by dividing the waveguide height by the mode number m :

$$125 \quad f_{cm} = \frac{mc}{2h} \quad (7)$$

126 Let $\tau = t - \frac{\rho}{c}$ be the time from the moment of arrival of the direct ray to the observer, then
 127 the instant frequency of Eq.(6) for the m^{th} order mode is given by (Yano *et al.*, 1989):

$$128 \quad f_m(\tau) = \frac{f_{cm}}{\sqrt{1 - \left(\frac{\rho}{\rho + c\tau}\right)^2}} \quad (8)$$

129 To compare the frequency dispersion in the spherical and flat models of the waveguide we
 130 use Eqs.(1-3). We define the instant frequency related to the middle of the interval between two
 131 successive rays: $T_n = (t_{n+1} + t_n)/2$ as a reciprocal of the delay between their arrivals:

$$132 \quad f(T_n) = \frac{1}{t_{n+1} - t_n}. \quad (9)$$

133 Fig.2(a) illustrates the calculation results of Eq.(9) for the first three modes, as plotted
 134 versus time $\tau_n = T_n - \rho/c$. The cutoff frequencies are shown by the horizontal dotted lines. The
 135 curves calculated for the spherical and flat waveguide models are combined, but the difference
 136 between them is hardly recognized in the graph. Fig.2(b) shows that the curves are the differences
 137 of instant frequencies $\Delta f = f_{\text{sphere}}(\tau_n) - f_{\text{flat}}(\tau_n)$. All the curves are calculated for distances $\rho =$
 138 1,2,3,4,5 Mm with the same waveguide height $h = 88$ km.

139 To use analytical representation of the instant frequency by Eq.(8) for the flat waveguide in
 140 the analysis of experimental data, we consider the “tail” part of a tweek waveform starting with delay
 141 τ_0 from the beginning of the tweek. By limiting the maximal deviation between the instantaneous
 142 frequencies by 10 Hz as seen in Fig.2(b) for practical use, we infer the following dependence of τ_0 on
 143 the source range:

$$144 \quad \tau_0 [\text{ms}] \cong 2\rho_0 [\text{Mm}]. \quad (10)$$

145 The initial estimation of the source range ρ_0 can be obtained by any appropriate known
 146 method. Exclusion of the “head” part of the tweek with fast varying instant frequency as is seen in
 147 Fig.2(a), will also facilitate the spectral-time analysis of experimental data.

148

149 3. Principles of estimation of ionospheric height and propagation distance of multimode tweek-
 150 atmospherics

151 Let $f_m(\tau)$ be the instant frequency of the m^{th} tweek harmonic extracted from the tweek trace in
 152 the spectrogram. The cutoff frequency can be estimated from Eq.(8):

$$153 \quad F_{cm}(\rho_1, \tau) = f_m(\tau) \sqrt{1 - \left(\frac{\rho_1}{\rho_1 + c\tau} \right)^2}. \quad (11)$$

154 Approaching ρ_1 in Eq.(11) to ρ , the propagation distance in the waveguide, will converge this
 155 dependence to a horizontal straight line at the cutoff frequency of $F_{cm}(\rho, \tau) = f_{cm}$. In order to find this
 156 solution we use a procedure of minimization of the absolute value of the slope b_m of the linear
 157 regression line ($r_m = a_m + b_m\tau$) for the dependence $F_{cm}(\rho_1, \tau)$ or minimization of the standard deviation
 158 σ_m from the mean value of $\langle F_{cm}(\rho_1, \tau) \rangle$.

159 When analyzing a multimode tweek we calculate $|b_m|$ for each of higher order tweek
 160 harmonics (Eq.(11)) separately and minimize the mean of the absolute values of the slope
 161 coefficients:

$$162 \quad \Phi(\mathbf{b}) = \frac{1}{M} \sum_{m=1}^M |b_m|. \quad (12)$$

163 The similar functional can be constructed to minimize the sum of the standard deviations of
 164 estimating the cutoff frequency in each mode.

165 In such a way that the inverse problem to find the two or more unknown parameters ρ and f_{cm}
 166 is reduced to the issue of one-dimensional optimization that gives us simultaneously all the cutoff
 167 frequencies for higher order modes and the source range ρ . Once we find the cutoff frequencies, the
 168 effective waveguide height for each mode is found from Eq.(7):

$$169 \quad h_m = \frac{mc}{2f_{cm}} \quad (13)$$

170 As was mentioned above there are some problems for the accurate measurement of the instant
 171 frequency of tweek-atmospherics, and one of them is the fast changing frequency in the beginning of
 172 a tweek signal. First, a method based on the compensation of the frequency dispersion in a tweek
 173 waveform was proposed by *Shimakura et al.* (1992) and *Hayakawa et al.* (1995). These authors
 174 constructed a “pseudo-spheric” which is a complex signal with the frequency modulation determined
 175 by the waveguide frequency dispersion defined by Eq.(6), and they multiplied it with the experimental
 176 record of the tweek. The amplitude spectrum of the resulting complex signal contains peaks at
 177 combination frequencies: the difference frequency and the summation frequency between the two
 178 multiplied signals. The difference frequency becomes equal zero and a straight line appears at zero
 179 frequency in the spectrogram after low pass filtration when the distance and waveguide height are
 180 found correctly and the instant frequencies of a tweek and the corresponding pseudo-spheric coincide
 181 with each other.

182 In this paper we consider this kind of transformation of the waveform of a tweek to
 183 compensate the waveguide frequency dispersion simultaneously for all harmonics by nonlinearly
 184 scaling a tweek along the time axis.

185 The arrival time of the reflected n^{th} ray with respect to the direct ray in the flat infinite
 186 waveguide, is given from Eq.(4):

$$187 \quad \tau_n = \sqrt{(2nh/c)^2 + (\rho/c)^2} - \rho/c. \quad (14)$$

188 Let $t_n = 2nh/c$ be the arrival time of n^{th} ray if the propagation were exactly perpendicular to the
 189 waveguide boundaries. Substituting t_n in Eq.(14) we can express t_n as a function of τ_n :

$$190 \quad t_n = \sqrt{\tau_n^2 + 2\tau_n(\rho/c)} \quad (15)$$

191 The moments t_n are proportional to n and it is obvious that they are equidistantly distributed
 192 along the time axis. By changing discrete quantities t_n and τ_n to continuous times t and τ in Eq.(15) we
 193 obtain the following continuous transformation of time:

$$194 \quad t_s = \sqrt{\tau^2 + 2\tau(\rho/c)} \quad (16)$$

195 The resultant transformation stretches the initial tweek waveform $w(\tau)$ and it is calculated from
196 the following expression:

$$197 \quad w_s [t_s(\tau, \rho)] = w(\tau). \quad (17)$$

198 After the transformation we expect maximization of peak amplitudes at the cutoff frequencies
199 in the amplitude spectrum of the stretched tweek w_s resulted from the equalization of delays between
200 successive rays.

201

202 4. Inverse problem solution for model atmospherics

203 To evaluate the effectiveness of our methods of estimation of the cutoff frequencies of the
204 Earth-ionosphere waveguide and the distance to a lightning discharge, tweek waveforms have been
205 synthesized using a simplified model of ELF-VLF propagation proposed by *Porrat et al.* (2001). The
206 horizontal magnetic component excited by a vertical electric dipole on the perfectly conducting
207 Earth's surface is expressed as the following modal sum [*Wait, 1962*]:

$$208 \quad H_\phi = j \frac{k I ds}{2h} \sum_{m=0}^{\infty} \delta_m S_m H_1^{(2)}(k S_m \rho), \quad (18)$$

209 where $I ds$ is the dipole current moment, h is the ionospheric height, k is the wavenumber in free
210 space, $H_1^{(2)}$ is the Hankel function of the second kind of the 1st order, S_m are the modal eigenvalues,
211 and δ_m , excitation factors. The source current moment is adopted as a single exponential pulse with

212 the spectrum $I ds(\omega) = \frac{I_0 \tau_1 ds}{1 + j\omega \tau_1}$ with appropriate parameters: $ds = 4\text{km}$, $I_0 = 20\text{kA}$, and $\tau_1 = 40\mu\text{s}$.

213 The SI units are used in the formulas throughout the paper unless explicitly mentioned.

214 The upper boundary, the ionosphere is described by an exponential conductivity profile with a
215 single scale height [*Wait and Spies, 1964*]:

$$216 \quad \sigma(z) = 2.5 \times 10^5 \varepsilon_0 e^{(z-H)/\zeta_0} \quad [\text{S/m}] \quad (19)$$

217 where ε_0 is the dielectric permittivity of vacuum, ζ_0 is the local scale height, z is the altitude above
 218 the ground, and H is the characteristic height of the profile.

219 For such a conductivity profile *Greifinger and Greifinger* [1978] have shown that the
 220 propagation in ELF range is determined by the lower “electrical” and higher “magnetic” heights. The
 221 lower altitude h_0 is the height at which the conduction current parallel to the magnetic field becomes
 222 equal to the displacement current, $\sigma(h_0) = \omega\varepsilon_0$. The upper altitude h_1 is the height at which the wave-
 223 like propagation turns into the diffusive penetration. It is determined by the condition equality of the
 224 local wave number to the reciprocal of the local scale height ζ_0 of the refractive index, $4\omega\mu_0\sigma(h_1)\zeta_0^2 =$
 225 1, which is considered as a “reflection altitude” [*Sentman*, 1990]. The frequency dependences for the
 226 altitudes h_0 and h_1 are obtained from the above conditions [*Nickolaenko and Rabinowicz*, 1982;
 227 *Nickolaenko and Hayakawa*, 2002]:

$$228 \quad \begin{aligned} h_0 &= H - \zeta_0 \ln \left(\frac{2.5 \times 10^5}{2\pi f} \right) \\ h_1 &= h_0 + 2\zeta_0 \ln \left(\frac{2.39 \times 10^7}{f\zeta_0} \right) = H + \zeta_0 \ln \left(\frac{1.44 \times 10^{10}}{f\zeta_0^2} \right) \end{aligned} \quad (20)$$

229 For the TEM mode in Eq.(18) $h = h_0(f)$, $\delta_0 = 1$, and the eigenvalue S_0 is given by [*Greifinger*
 230 *and Greifinger*, 1978]:

$$231 \quad S_0^2 = \frac{h_1 + j \frac{\pi}{2} \zeta_0}{h_0 - j \frac{\pi}{2} \zeta_0} \quad (21)$$

232 The higher order modes of tweeks are represented mainly by quasi-TE modes resulted from
 233 the coupling of TM waves excited by a vertical dipole into TE waves due to the reflection from the
 234 anisotropic ionosphere during night time [*Yamashita*, 1978; *Sukhorukov et al.*, 1992; *Sukhorukov*,
 235 1996]. For the higher order modes in Eq.(18) $h = h_1(f)$, the eigenvalues and the excitation factors are
 236 given by [*Porrot et al.*, 2001]:

$$\begin{aligned}
237 \quad S_m &\approx s_m + j \frac{\pi \zeta_0}{2h_1} \frac{c_m^2}{s_m}, \quad \delta_m \approx 2 \frac{c_m^2}{s_m}, \quad f > \sqrt{2} f_{cm} \\
S_m &\approx s_m + j \frac{\pi \zeta_0}{2h_1} s_m, \quad \delta_m \approx 2s_m, \quad f < \sqrt{2} f_{cm}
\end{aligned} \tag{22}$$

238 where f_{cm} is the cutoff frequency of m^{th} mode, $c_m = m\pi / kh_1$ and $s_m = \sqrt{1 - c_m^2}$ are the modal cosine
239 and sine.

240 The waveforms of tweeks were obtained by applying the inverse FFT to the modeled spectra.
241 In the further modeling we calculated the spectra of magnetic field component consisting of nine
242 modes including the zero order one.

243 An example of such a synthesized waveform and its amplitude and dynamic spectrum are
244 shown in Fig.3(a-c). The model parameters are adopted as follow: $H = 88$ km, $\zeta_0 = 1.67$ km, $\rho = 1600$
245 km.

246 In order to retrieve the time dependences of the instant frequencies of tweek harmonics we
247 calculated a moving-window spectrum of the tweek waveform with 5.12 ms Hamming window
248 length with a step of 0.5 ms starting from the moment delayed by τ_0 from the pulse onset calculated
249 by Eq.(10). The starting point τ_0 is marked by a triangle on the lower time axis. The peak frequencies
250 were defined more accurately by means of interpolation with a parabola inscribed to the point of a
251 spectral maximum and two adjacent points. The inferred peaks in the dynamic spectrum
252 corresponding to the first five higher order modes are shown in Fig.3(c) by small circles.

253 The stretched waveform transformed with Eqs. (16) and (17) and its amplitude spectrum are
254 illustrated in Fig.4. To apply the FFT to the data we uniformly resampled the stretched tweek
255 waveform using linear interpolation. We can observe that the intermodal interference practically
256 disappears and the spectrum of the transformed tweek waveform consists of the peaks at the cutoff
257 frequencies corresponding to separate modes.

258 The pairs of instant frequencies $f_m(\tau)$ and corresponding delays τ retrieved from a dynamic
259 spectrum are used to estimate cutoff frequencies in the first method described in Section 3. Fig. 5
260 demonstrates the fitting procedure to obtain the effective waveguide from higher order tweek

261 harmonics of the synthesized tweek waveform shown in Fig.3. Instead of estimating cutoff
 262 frequencies from Eq.(12) in this figure we plot the effective waveguide heights given by: $h_m(\rho, \tau) =$
 263 $cm/2F_m(\rho, \tau)$. The model effective heights $h_1(f_{cm})$ theoretically calculated, are shown by the horizontal
 264 dotted lines labeled with the corresponding mode numbers. Cases of an underestimated propagation
 265 distance, $\rho = 1500$ km, the exact propagation distance, $\rho = 1600$ km, and an overestimated
 266 propagation distance, $\rho = 1700$ km are treated in Fig.4(a,b,c) respectively.

267 We can observe that the points are to be grouped horizontally around certain altitudes when
 268 the source-to-observer distance is set correctly. The parameter h_1 is logarithmically decreasing with an
 269 increase with frequency as it follows from Eq.(20) and then the effective waveguide height $h_1(f_{cm})$
 270 decreases with increasing the mode number in the adopted model of propagation for the synthesized
 271 tweek. Note that underestimation of the source range leads to underestimation of the waveguide
 272 height and vice versa.

273 For the stretched tweek shown in Fig.4, we demonstrate the second method to determine the
 274 waveguide height and the propagation distance. With the help of the proposed transformation we
 275 compensate the frequency dispersion in the individual modes, when the parameter ρ equals to the
 276 factual value of the source range. For the stretched waveform, we can extend the length of a window
 277 to construct a moving-window spectrum and hence we can improve the estimation of the cutoff
 278 frequency and of the source range and the waveguide height.

279 We demonstrate the fitting procedure for the stretched tweek waveform so as to obtain the
 280 effective waveguide height for higher order modes by varying the source range ρ in Fig.6 just like that
 281 shown in Fig.5 in the case of the first method. The cases of an underestimated range, $\rho = 1500$ km, the
 282 exact range, $\rho = 1600$ km, and an overestimated range, $\rho = 1700$ km are shown in Fig.6(a,b,c)
 283 respectively. We can observe a smaller deviation in the estimations of effective heights in comparison
 284 with the nonstretched one (see Fig.5(a-c)) due to a larger moving window length, of about 15 ms used
 285 for constructing a dynamic spectrum.

286

287 5. Estimation of the accuracy and application to experimental records

288 In order to evaluate the accuracy of our proposed methods we synthesized atmospheric
289 waveforms of 20 ms length for source range from 500 to 3500 km. For these distances we expect to
290 observe two or more harmonics in the experimental records of tweeks [*Outsu, 1960; Gorishnya and*
291 *Shvets, 2010*] that can be used for estimating the cutoff frequencies of the Earth-ionosphere
292 waveguide. Together with the first and second methods described earlier for comparison we also
293 apply the third “sonogram” method (see e.g. *Ohya et al., 2008*) based on the optimization of two
294 parameters in such a way that the theoretical dependence of the instantaneous frequency Eq.(18) fits
295 to the trace in the spectrogram of a tweek. In the last case we determine a pair of parameters, the
296 source range and the waveguide height, separately for each tweek of harmonics.

297 In the simulation a white noise was generated by random values following a normal
298 distribution with zero mean and standard deviation 0.2 of the standard deviation σ of the analyzed part
299 of a tweek signal. For each distance of 500, 1500, 2500 and 3500 km we synthesized tweek
300 waveforms with the following parameters of the ionosphere conductivity profile: $H = 88$ km, $\zeta_0 = 1.67$
301 km. Then noise realizations generated independently were added to them and the required parameters
302 were calculated. This process was repeated 100 times for each distance. Tables 1 and 2 present the
303 overall systematic errors calculated as a difference between the mean value of 100 tests and the model
304 parameter together with the standard deviations for the found distances and heights for different
305 modes.

306 We can see from the tables that the errors mainly decrease with an increase in the mode
307 number for all methods, which can be connected with an increase in the relative accuracy of the
308 frequency estimation for the higher order modes. As it follows from Tables 1 and 2, while the first
309 and third methods exhibit the concurring accuracy, the second method is found to demonstrate about
310 two times better results in the estimation of the source range and waveguide height.

311 Examples of estimation of the effective height and the propagation path length by using
312 experimental records of tweeks are demonstrated in Fig.7. Two horizontal magnetic and a vertical

313 electric components, received in the frequency range 0.3 – 13 kHz, were recorded digitally with the
314 sampling frequency of 100 kHz. The records were made at different places onboard the scientific
315 vessel “Academician Vernadsky” in 1991 (more experimental details are given in *Shvets and*
316 *Hayakawa* [1998]).

317 Analysis results of the experimental records are presented with the use of the second technique
318 described above. Tweek waveforms of magnetic components were decomposed into transversal and
319 longitudinal components with reference to the source direction (see *Rafalsky et al.* 1995) and we
320 analyzed the longitudinal component which is composed only by higher-order modes. Fig.7 illustrates
321 the waveforms, amplitude spectra and estimated effective heights for different waveguide modes of
322 the tweeks recorded at 5.55° E, 16.7° S on January 21, 1991 (a, b) and at 3.6° W, 8° S on April 10,
323 1991(c, d). We also indicate the parameters of the exponential ionospheric conductivity profile H and
324 ζ_0 , the distance to the source ρ and the source azimuth α counted clockwise from North direction are
325 shown below the corresponding graphs. The circle points with the standard deviation bars denote
326 experimentally found effective heights on the right-most graphs and the solid line is the fitted
327 theoretical dependence of h_1 Eq.(20) which yields the estimated parameters H and ζ_0 . We have chosen
328 two tweeks arrived from approximately the same direction but from different distances on each day.
329 We should note that in the examples presented of tweek analysis the waveguide height decreases with
330 increasing the mode number, which is basically in agreement with the models by Sukhorukov et al.
331 [1992a,b] and Porrat et al. [2001]. It is also found that estimations of the waveguide height and the
332 reconstructed conductivity profile parameters are quite close for each pair of tweeks that can indicate
333 quiet ionospheric conditions along the corresponding propagation paths.

334

335 6. Summary and conclusion

336 Both of the proposed techniques for estimating the waveguide cutoff frequencies described in
337 the previous two sections are based on linearizing transformations that compensate the waveguide
338 frequency dispersion of tweek harmonics.

339 Algorithms of the estimations of Earth-ionosphere waveguide parameters for the above-
340 described techniques are formulated as follows:

341 First technique:

342 1) calculation of dynamic spectrum;

343 2) selection of tweek harmonics;

344 3) minimization of the functional (12) by seeking an optimal value of the propagation distance,
345 that includes the calculation of the slope of the regression lines of the cutoff frequency estimations in
346 selected tweek harmonics Eq.(11).

347 Second technique:

348 1) minimization of functional (12) by seeking an optimal value of the propagation distance,
349 that includes:

350 i) rescaling the tweek waveform with a new value of ρ by transformations of Eqs. (16, 17);

351 ii) calculation of dynamic spectrum;

352 iii) selection of tweek harmonics;

353 iv) calculation of the slope of the regression lines of the cutoff frequency estimations in
354 selected tweek harmonics.

355 As we can see, the second algorithm requires much more computer resource and so is time-
356 consuming in comparison to the first method. It includes rescaling a tweek, calculating its dynamic
357 spectrum and selecting tweek harmonics in each cycle of seeking an optimal value of ρ , whereas the
358 calculation of the dynamic spectrum and selecting tweek harmonics are performed only once in the
359 first algorithm. However, the second algorithm has essential advantage in the estimation accuracy of
360 waveguide parameters due to an increased frequency resolution of the moving-window spectral
361 processing.

362 As a conclusion of this study we note the following.

363 An approach has been proposed that reduces the problem of finding two or more unknown
364 parameters, source range and cutoff frequencies, by using higher harmonic tweeks to an issue of one-
365 dimensional optimization.

366 A new technique has been proposed, based on the nonlinear scaling of a tweek waveform
367 along the time axis that compensates the waveguide frequency dispersion in the signal and allows us
368 to improve the accuracy of estimation of the waveguide cutoff frequencies, especially in the presence
369 of noises.

370 Limitations of the use of dispersion relation for a flat waveguide model to the spherical
371 waveguide have been elaborated.

372 Based on the numerical modeling of multimode tweek-atmospherics in the nocturnal Earth-
373 ionosphere waveguide with exponential vertical conductivity profile of the lower ionosphere (Porrat
374 et al., 2001), it was shown that the accuracy of estimating the effective ionosphere height is good
375 enough, about 100-400 m for the first and higher order modes in a case of signal-to-noise ratio of
376 being 5 in the modeled tweeks. It enables us to deduce the parameters of vertical conductivity profile
377 of the lower ionosphere for a wide range of source-to-observer distance from a few hundred to a few
378 thousand kilometers, as long as two or more tweek harmonics can be detected.

379 Examples of analyses of experimental records of tweeks are found to indicate a decrease in the
380 effective height of the waveguide with increasing the mode number. Estimated scale height of the
381 exponential conductivity profile of the isotropic lower ionosphere model is found to be in a range of
382 0.4 – 2.5 km.

383

384 Acknowledgement. A. V. S. and T. M. S. are grateful to the University of Electro-Communications
385 for offering an opportunity for collaborative research in the University.

386

387

388

References

- 389 Cummer, S.A., U.S. Inan, and T.F. Bell, Ionospheric D-region remote sensing using VLF radio
390 atmospherics. *Radio Sci.*, 33, 1781-1792, 1998.
- 391 Cummer, S.A., Modeling electromagnetic propagation in the Earth-ionosphere waveguide. *IEEE*
392 *Trans. Ant. Prop.*, 48, 1420-1429, 2000.
- 393 Gorishnya, Y.V., and A.V. Shvets, Statistical study of multimodal tweek-atmospherics,
394 *Mathematical Methods in Electromagnetic Theory (MMET)*, 2010 International Conference on
395 6-8 Sept. 2010, P.98-101, 10.1109/MMET.2010.5611445, 2010.
- 396 Greifinger, C., and P. Greifinger, Approximate method for determining ELF eigenvalues in the
397 earth-ionosphere waveguide. *Radio Sci.*, 13(5), 831-837, 1978.
- 398 Hayakawa, M., K. Ohta, and K. Baba, Wave characteristics of tweek atmospherics deduced from the
399 direction finding measurement and theoretical interpretations, *J. Geophys. Res.*, 99, 10733-10743,
400 1994.
- 401 Hayakawa, M., K. Ohta, S. Shimakura, and K. Baba, Recent findings on VLF/ELF spherics, *J.*
402 *Atmos. Terr. Phys.*, 57, No 5, 467-477, 1995.
- 403 Maurya, A. K., B. Veenadhari, R. Singh, S. Kumar, M. B. Cohen, R. Selvakumaran, S. Gokani, P.
404 Pant, A. K. Singh, and U. S. Inan, Nighttime D region electron density measurements from
405 ELF-VLF tweek radio atmospherics recorded at low latitudes, *J. Geophys. Res.*, 117, A11308,
406 doi:10.1029/2012JA017876, 2012.
- 407 Mikhailova G.A., and O.V. Kapustina, The frequency-time structure of “tweek”-type atmospherics
408 and VLF diagnostics of parameters of the night-time lower ionosphere, *Geomagn. Aeron.*, 28,
409 879-882, 1988.
- 410 Nickolaenko, A.P. and L.M. Rabinowicz, On the possibility of the global electromagnetic
411 resonances on the planets of Solar system, *Kosmicheskie Issledovasniya (Space Research)*, 20,
412 No. 1, 82–87, 1982 (in Russian).

- 413 Nickolaenko, A.P., and M. Hayakawa, Resonances in the Earth-Ionosphere Cavity, Kluwer Acad.
414 Pub., Dordrecht, 380p, 2002.
- 415 Nickolaenko, A.P., V.A. Rafalsky, A.V. Shvets, and M. Hayakawa, A time domain direction
416 finding technique for locating wide band atmospherics, *J. Atmos. Electr.*, 14, No 1, 97-107, 1994.
- 417 Ohya, H., K. Shiokawa, and Y. Miyoshi, Development of an automatic procedure to estimate the
418 reflection height of tweek atmospherics, *Earth Planets Space*, 60, 837–843, 2008.
- 419 Otsu, J., Numerical study of tweeks based on wave-guide mode theory, *Proc. Res. Inst. Atmos.*,
420 Nagoya Univ., 7, 58-71, 1960.
- 421 Porrat, D., P. R. Bannister, and A. C. Fraser-Smith, Modal phenomena in the natural electromagnetic
422 spectrum below 5 kHz, *Radio Sci.*, 36, 499–506, 2001.
- 423 Rafalsky, V.A., A.P. Nickolaenko, A.V. Shvets, and M. Hayakawa, Location of lightning discharges
424 from a single station, *J. Geophys. Res.*, 100, D10, P. 20,829-20,838, 1995.
- 425 Ryabov, B.S., Tweek formation peculiarities in the Earth-ionosphere waveguide and low ionosphere
426 parameters, *Adv. Space Res.*, 12(6), 255 – 258, 1992.
- 427 Sentman, D.D., Approximate Schumann resonance parameters for a two-scale-height ionosphere, *J.*
428 *Atmos. Terr. Phys.*, 52(1), 35 – 46, 1990.
- 429 Shvets, A. V., and Y.V. Gorishnyaya, The method of location of lightning and evaluation of
430 parameters of bottom ionosphere with the help of tweek-atmospherics, *Radiophysics and*
431 *Electronics*, 15, № 2, 63-70, 2010.
- 432 Shvets, A.V., and M. Hayakawa, Polarization effects for tweek propagation, *J. Atmos. Solar-Terr.*
433 *Phys.*, 60, No 4, 461–469, 1998.
- 434 Shimakura, S., Y. Honga, and M. Hayakawa, Measurement of the ionospheric height and
435 propagation distance on the basis of dispersion properties of tweek atmospherics, *Proceedings of*
436 *ISAP '92, SAPPORO, JAPAN*, 501-504, 1992.
- 437 Sukhorukov, A.I., ELF-VLF atmospheric waveforms under night-time ionospheric conditions. *Ann.*
438 *Geophys.*, 14, 33-41, 1996.

- 439 Sukhorukov, A. I., Approximate solution for VLF propagation in an isotropic exponential earth-
 440 ionosphere waveguide. *J. Atmos. Terr. Phys.*, 55(6), 919 – 930, 1993.
- 441 Sukhorukov, A.I., S. Shimakura, and M. Hayakawa, On the additional dispersion of a whistler in
 442 the earth-ionosphere waveguide, *Planet. Space Sci.*, 40(9), 1185-1191, 1992a.
- 443 Sukhorukov, A.I., S. Shimakura, and M. Hayakawa, Approximate solution for the VLF eigenvalues
 444 near cut-off frequencies in the nocturnal inhomogeneous earth-ionosphere waveguide, *Planet.*
 445 *Space Sci.*, 40(10), 1363-1369, 1992b.
- 446 Wait, J.R., *Electromagnetic Waves in Stratified Media*, Pergamon Press, New York, 1962.
- 447 Wait, J.R. and K.P. Spies, Characteristics of the earth-ionosphere waveguide for VLF radio waves.
 448 Technical Note 300, *National Bureau of Standards*, December 1964.
- 449 Yamashita, M., Propagation of tweek atmospherics, *J. Atmos. Terr. Phys.*, . 40, 151-156, 1978.
- 450 Yano. S., T. Ogawa, and H. Hagino, Waveform analysis of tweek atmospherics, *Res. Lett. Atmos.*
 451 *Electr.*, 9, 31-42, 1989.
- 452 Yedemsky, D.Ye., B.S. Ryabov, A.Yu. Shchokotov, and V.S. Yarotsky, Experimental investigation
 453 of the tweek field structure, *Adv. Space Res.*, 12, No 6, 251-254, 1992.

454 Figure and Table captions

455 Fig.1. Ray paths in the spherical waveguide (Adapted from Yano et al., 1989).

456 Fig.2. (a) Calculated traces of a tweek and (b) difference of instant frequencies $\Delta f = f_{\text{sphere}}(\tau) - f_{\text{flat}}(\tau)$
 457 between the spherical and flat waveguide models .

458 Fig. 3. Waveform (a), amplitude (b), and dynamic spectrum (c) of a modeled tweek-atmospheric
 459 calculated for the following parameters: $H = 88$ km, $\zeta_0 = 1.67$ km, $\rho = 1600$ km. The vertical dotted
 460 lines in the amplitude spectrum (b) indicate the cutoff frequencies.

461 Fig. 4. (a) The stretched waveform, and (b) its amplitude spectrum of the modeled tweek-atmospheric
 462 shown in Fig.3. The vertical dotted lines on the amplitude spectrum (b) indicate the cutoff
 463 frequencies.

464 Fig. 5. Estimation of the effective waveguide heights for higher order modes, $m=1 \dots 5$ from (Eq.(6))
465 of a modeled tweek-atmospheric shown in Fig 3(a). Horizontal dotted lines show the effective heights
466 calculated from the model. Three cases are dealt with; (a) underestimated range, $\rho = 1500$ km, (b)
467 exact range, $\rho = 1600$ km, (c) overestimated range, $\rho = 1700$ km.

468 Fig. 6. Estimation of the effective heights of the Earth-ionosphere waveguide obtained from the
469 stretched tweek waveform shown in Fig.4(a). Horizontal dashed lines show the effective heights for
470 the corresponding modes. a) underestimated range, $\rho = 1500$ km, b) exact range, $\rho = 1600$ km, c)
471 overestimated range, $\rho = 1700$ km.

472 Fig.7. Waveforms, amplitude spectra and estimated effective heights for different waveguide modes
473 for the tweeks recorded at 5.55° E, 16.7° S on January 21, 1991 (a, b) and at 3.6° W, 8° S on April 10,
474 1991(c, d). Estimated parameters of the exponential ionospheric conductivity profile H and ζ_0 , the
475 distance to the source ρ and the source azimuth α counted clockwise from North direction are shown
476 below the corresponding graphs. The circle points with the standard deviation bars denote
477 experimentally found effective heights on the right-most graphs and the solid line is the fitted
478 theoretical dependence of h_1 Eq.(20) which yields the estimated parameters H and ζ_0 .

479 Table 1 Errors of estimations of the source distance.

480 Table 2 Errors of estimations of the waveguide effective height.

481

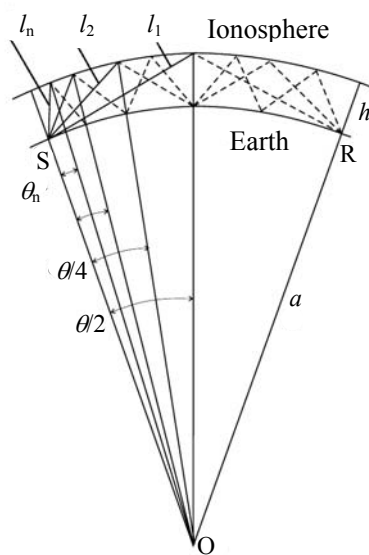


Fig.1.

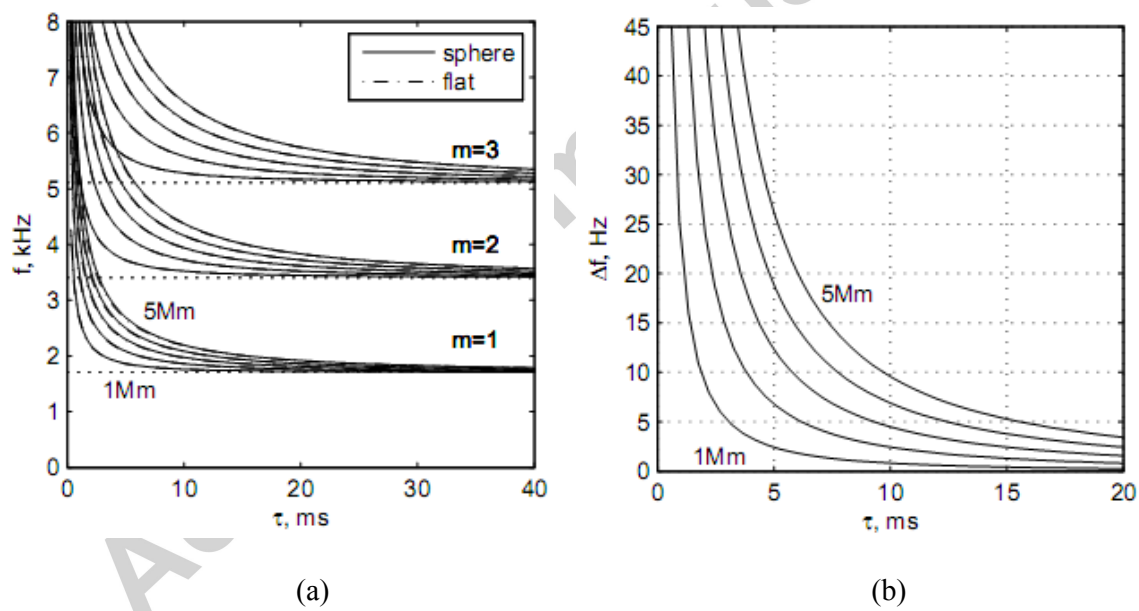
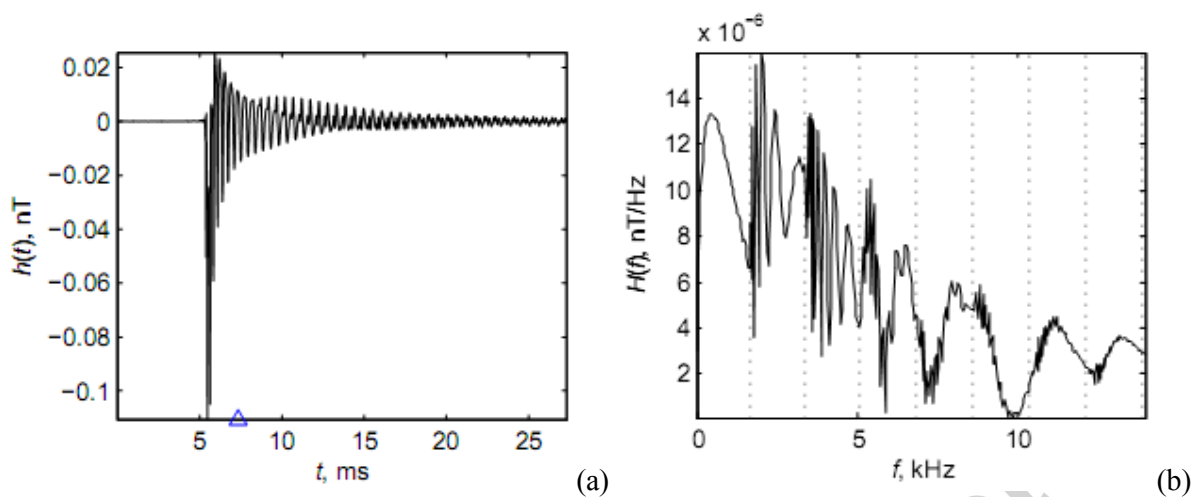
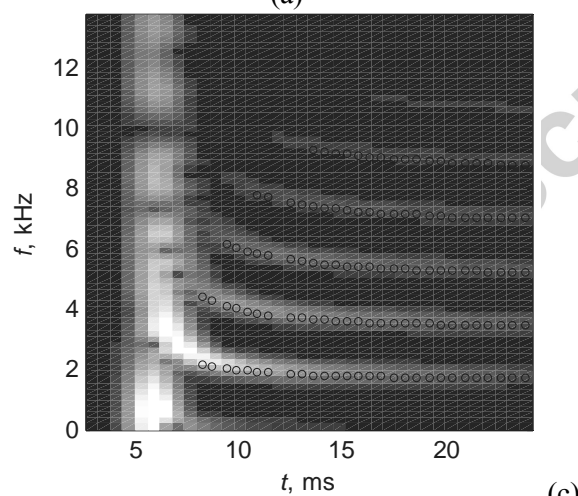


Fig.2.

488



489



(c)

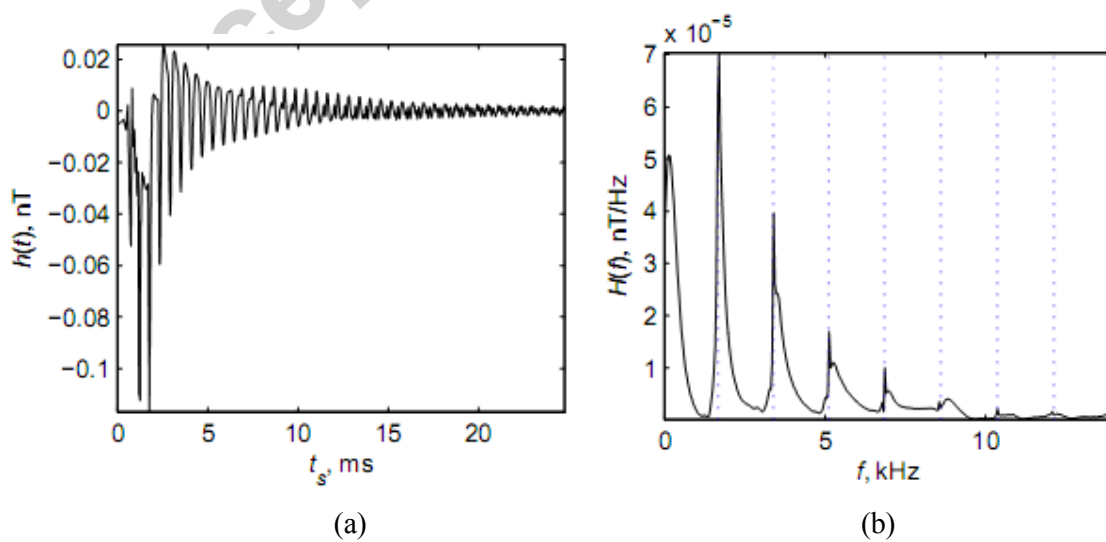
490

491

492

Fig. 3.

493



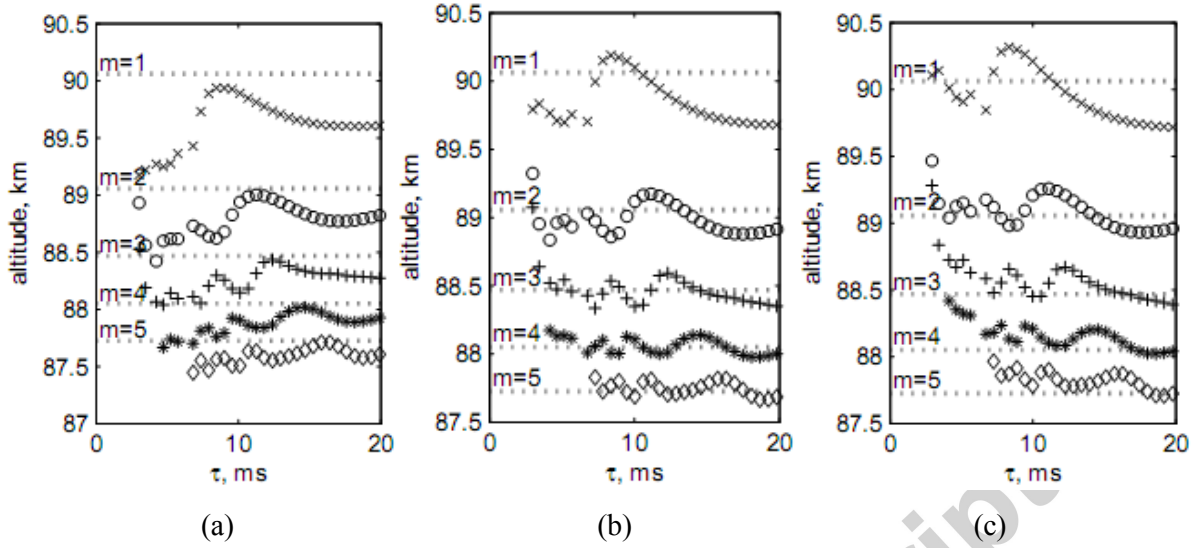
494

495

496

Fig. 4.

497

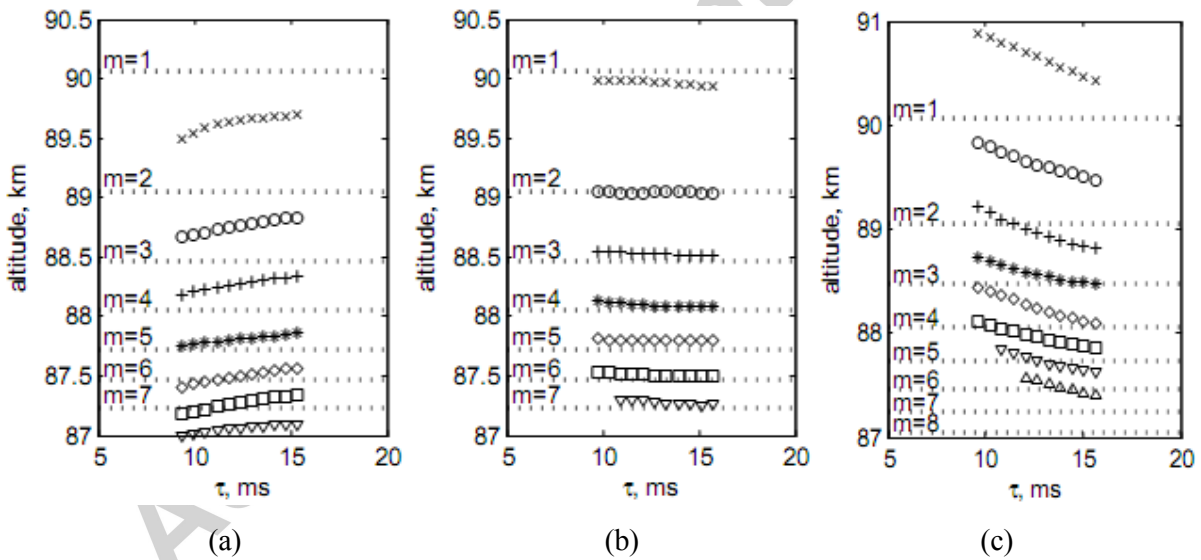


498

499

500 Fig. 5.

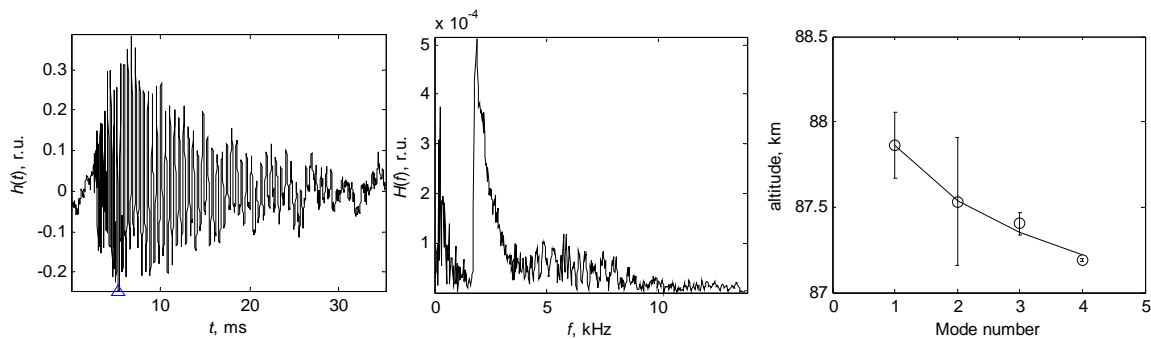
501



502

503

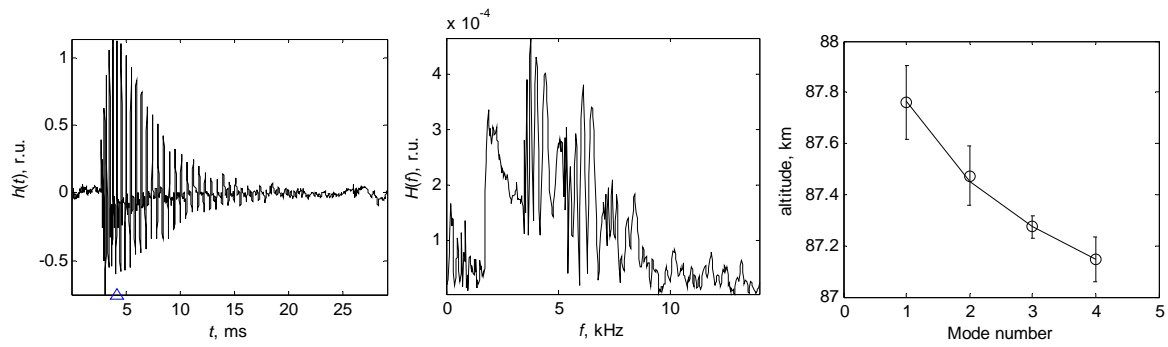
504 Fig. 6.



505

506

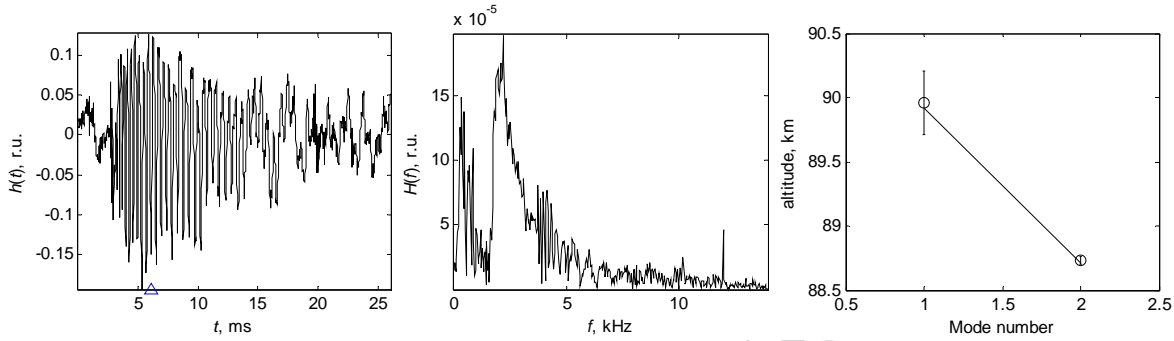
a) 21-Jan-1991, 20:30:47 UT, $\rho=2.55$ $\alpha=62.9^\circ$, $H=86.2$ km, $\zeta_0=0.46$ km.



507

508

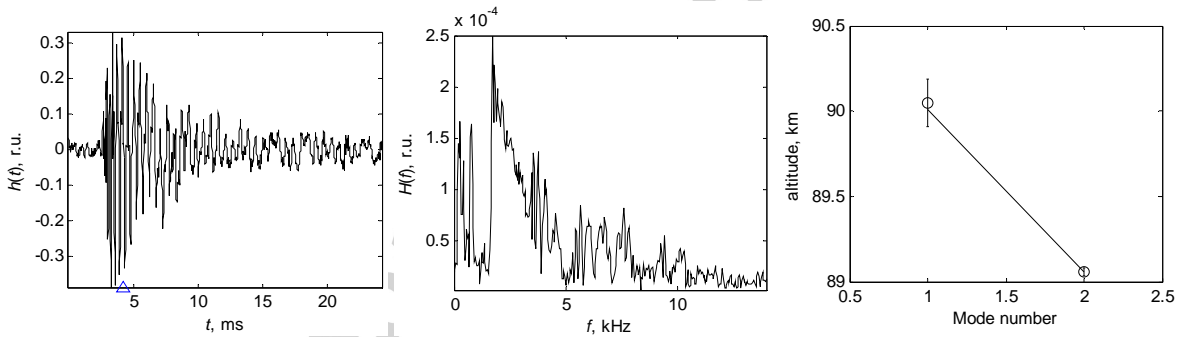
b) 21-Jan-1991, 20:29:22 UT, $\rho = 1.19$ Mm, $\alpha = 78.6^\circ$, $H = 86.1$ km, $\zeta_0 = 0.44$ km.



509

510

c) 10-Apr-1991, 01:30:20 UT, $\rho = 2.68$ Mm, $\alpha = 279.3^\circ$, $H = 88.1$ km, $\zeta_0 = 1.72$ km.



511

512

513

d) 10-Apr-1991, 01:24:39 UT, $\rho = 1.09$ Mm, $\alpha = 276.7^\circ$, $H = 88.0$ km, $\zeta_0 = 1.41$ km.

Fig.7.

514

515 Table 1. Errors of estimations of the source distance.

ρ , km	Method 1		Method 2		Method 3	
	Syst. error, km	Std. dev., km	Syst. error, km	Std. dev., km	Syst. error, km	Std. dev., km
500	-18	22	5	9	-30	44
750	10	37	11	10	2	45
1500	18	18	13	26	15	56
2500	55	27	42	49	65	56
3500	207	59	45	42	148	112

516

517 Table 2. Errors of estimations of the waveguide effective height.

Mode #	Method 1		Method 2		Method 3	
	Syst. error, m	Std. dev., m	Syst. error, m	Std. dev., m	Syst. error, m	Std. dev., m
$\rho = 500$ km						
1	-225	757	-375	175	-24	1371
2	-95	315	-27	64	76	437
3	-2	207	-74	99	152	231
4	-49	232	-11	54	-17	262
5	-10	179	-37	40	-47	148
$\rho = 1500$ km						
1	-335	151	-241	169	-272	244
2	-80	108	-44	112	-110	69
3	-84	93	39	167	-72	90
4	-52	76	51	115	-55	135
5	-62	137	46	114	-43	476
$\rho = 2500$ km						
1	-219	131	-267	270	13	52
2	-108	125	-77	181	-319	89
3	-100	93	-32	237	-220	197
$\rho = 3500$ km						
1	-657	247	-204	190	-5	58
2	-565	191	-50	130	-713	244

518

519

520 Table 1. Errors of estimations of the source distance.

ρ , km	Method 1		Method 2		Method 3	
	Syst. error, km	Std. dev., km	Syst. error, km	Std. dev., km	Syst. error, km	Std. dev., km
500	-18	22	5	9	-30	44
750	10	37	11	10	2	45
1500	18	18	13	26	15	56
2500	55	27	42	49	65	56
3500	207	59	45	42	148	112

521

522 Table 2. Errors of estimations of the waveguide effective height.

Mode #	Method 1		Method 2		Method 3	
	Syst. error, m	Std. dev., m	Syst. error, m	Std. dev., m	Syst. error, m	Std. dev., m
$\rho = 500$ km						
1	-225	757	-375	175	-24	1371
2	-95	315	-27	64	76	437
3	-2	207	-74	99	152	231
4	-49	232	-11	54	-17	262
5	-10	179	-37	40	-47	148
$\rho = 1500$ km						
1	-335	151	-241	169	-272	244
2	-80	108	-44	112	-110	69
3	-84	93	39	167	-72	90
4	-52	76	51	115	-55	135
5	-62	137	46	114	-43	476
$\rho = 2500$ km						
1	-219	131	-267	270	13	52
2	-108	125	-77	181	-319	89
3	-100	93	-32	237	-220	197
$\rho = 3500$ km						
1	-657	247	-204	190	-5	58
2	-565	191	-50	130	-713	244

523

524

525

526 **Highlight**

527 *Three techniques are evaluated to find source range and ionosphere height by
528 multimode tweeks.

529 *Curve-fitting problem for two or more parameters is simplified to one parameter
530 optimization.

531 *A new technique is proposed based on a nonlinear transformation of tweek
532 waveform.

533 *Analysis of tweek records shows decreasing ionosphere height with increase of
534 mode number.

535 *Parameters of the exponential conductivity profile of the ionosphere are
536 estimated by tweeks.

Accepted manuscript